Journal of Integrative Neuroscience

J. Integr. Neurosci. **2026**; 25(3): 44233
https://doi.org/10.31083/JIN44233

Original Research

Analysis of Electroencephalogram Characteristics in Patients with Varying Degrees of Disorders of Consciousness

Yanhua Shi[1,2,†], Siyu Long[1,2,†], Wenjun You[3], Jing Zhu[1], Jiawen Chen[1,2], Mengyu Zhou[1,2], Jie Gao[1,*], Su Liu[1,2,*]

[1]Department of Rehabilitation Medicine, Affiliated Hospital of Nantong University, 226001 Nantong, Jiangsu, China
[2]School of Nursing and Rehabilitation, Nantong University, 226001 Nantong, Jiangsu, China
[3]Department of Geriatrics, Affiliated Nantong Rehabilitation Hospital of Nantong University, 226001 Nantong, Jiangsu, China
*Correspondence: gaojie230@163.com (Jie Gao); 327202278@qq.com (Su Liu)
[†]These authors contributed equally.
Academic Editor: Bettina Platt
Submitted: 24 June 2025 Revised: 8 January 2026 Accepted: 16 January 2026 Published: 25 March 2026

Abstract

Background: The subjective limitations of neurobehavioral assessment cause a high misdiagnosis rate for disorders of consciousness (DoC). The purpose of this study was to identify the DoC level based on an analysis of multi-dimensional electroencephalogram (EEG) signals to assist with establishing a clinical diagnosis. **Methods**: Sixty-seven patients with DoC [coma, n = 19; vegetative state (VS), n = 23; and minimally conscious state (MCS), n = 25] were included to analyze resting state EEG characteristics. The EEG features were statistically compared among five band powers (delta, theta, alpha, beta, and gamma) and five brain regions (prefrontal, frontal, parietal, temporal, and occipital) by multidimensional analyses, including time-domain analysis, spectral analysis, and functional brain connectivity. **Results**: Amplitude-integrated electroencephalography (aEEG) center amplitude showed significant differences between coma and MCS ($p = 0.02688$), with no significant differences observed for the other comparison. Spectral analysis revealed that delta and theta power decreased with higher consciousness levels, whereas alpha, beta, and gamma power increased. Relative power differed among groups across specific brain regions (prefrontal, frontal, parietal, temporal, and occipital) and frequency bands. Weighted Phase Lag Index (wPLI) based functional connectivity demonstrated frequency-specific network reorganization with theta band connectivity strongest in VS and alpha/beta/gamma band connectivity enhanced in MCS. Absolute power topographic maps showed expanding high-power regions from coma-to-MCS in high-frequency bands and the left dorsolateral prefrontal cortex (DLPFC) (F3 electrode) exhibited a consistent power gradient of coma $<$ MCS $<$ VS across all bands. **Conclusions**: Multidimensional EEG features have significant value in differentiating the levels of consciousness disorders. aEEG center amplitude discriminated MCS from coma; delta/gamma relative power separated VS from MCS, and alpha/beta relative power separated coma, VS, and MCS. Parieto-occipital connectivity matrix in the theta band distinguishes coma from VS, while absolute power topography of the left DLPFC shows potential for grading levels of impaired consciousness. These electrophysiologic biomarkers complement behavioral assessments, enhancing diagnostic accuracy.

Keywords: disorders of consciousness; electroencephalogram; spectrum analysis

1. Introduction

Disorders of consciousness (DoC) refer to a spectrum of conditions characterized by impaired levels of consciousness due to various underlying causes. DoC are primarily classified into coma, vegetative state (VS), and minimally conscious state (MCS) [1]. Despite advances in clinical practice, accurately determining the specific level of consciousness in DoC patients remains a significant challenge. The precise assessment and differentiation between these states are crucial for guiding diagnosis and treatment but continue to present difficulties in the management of DoC patients.

Several standardized assessment methods have been developed specifically for evaluating DoC patients, among which the Coma Recovery Scale-Revised (CRS-R) is widely recognized for its practicality and effectiveness. The CRS-R is particularly sensitive in detecting the MCS, making the CRS-R a valuable tool in the assessment of DoC patients. However, the reliability of these neurobehavioral measures can be compromised due to the subjective nature of the evaluation process, resulting in variable accuracy of the assessment outcomes [2]. Therefore, while neurobehavioral scales are useful for diagnosing DoC, neurobehavioral scales are not entirely dependable.

Neuroimaging techniques, such as functional Magnetic Resonance Imaging (fMRI) and Positron Emission Tomography (PET), provide objective assessment of DoC by probing underlying brain function, detecting covert awareness, and revealing behaviorally undetectable neural correlates of consciousness [3,4]. However, routine clinical use of neuroimaging techniques is significantly limited by high costs, restricted accessibility, technical demands (e.g., patient transport and MRI compatibility), and challenges in scanning critically ill patients [5]. In contrast,

electroencephalogram (EEG)-based approaches offer substantial advantages, including bedside monitoring of spontaneous brain activity, delivering high temporal resolution, portability, repeatability, and lower cost [6]. Advances in EEG analysis enhance diagnostic accuracy and covert consciousness detection [7,8], making EEG a critical tool for complementing behavioral and neuroimaging assessments. Within the EEG methodologies, amplitude-integrated EEG (aEEG) presents a streamlined solution. aEEG compresses raw EEG data into min-max amplitude bands on a semi-log scale, enabling rapid visual trend assessment [9]. Although originally developed for neonatal monitoring [9], the artifact tolerance, simplicity, and suitability of aEEG for continuous monitoring facilitate effective translation to adult critical care [10], for which aEEG is gradually being applied.

EEG signals are classified into low-frequency bands, including delta, theta, and alpha, as well as high-frequency bands, such as beta and gamma. The brain activity state is assessed based on the amplitude and fluctuations of EEG waveforms. Under normal awake conditions EEG amplitudes and waveforms exhibit regular patterns. However, the spectral power across these frequency bands is significantly disrupted in patients with DoC [11]. Klimesch [12] reported that variations in alpha and theta reflect cognitive function and memory capabilities. Patients with DoC typically display enhanced delta and suppressed alpha compared to healthy individuals [5]. Naro *et al.* [13] further noted that patients with MCS exhibit higher power in theta and alpha than patients with VS in whom alpha wave activity is closely associated with consciousness recovery. Specifically, alpha power in the parietal and occipital regions is significantly increased in patients with MCS [13,14]. In addition, Piarulli *et al.* observed that beta power is notably higher in patients with MCS compared to patients with VS. However, research on high-frequency bands, such as beta and gamma in DoC, is limited [15].

Consciousness-related information in the brain is often complex and multifaceted. The spectral power of EEG and the amplitude changes in specific frequency bands reflect the differences and correlations between various states of consciousness. Numerous studies have examined the relationship between EEG and consciousness states and shown that consciousness is not simply a "present or absent" condition. EEG-based neurofunctional imaging techniques offer an innovative approach to tackling this challenge. Cavinato *et al.* [16] observed that patients in a VS exhibit impaired cortical integration with significant disruption of the associations between the frontal and parietal lobes. In contrast, Wu *et al.* [17] reported that patients in a MCS exhibit superior functional connectivity between brain regions with enhanced cortical peripheral connectivity compared to patients with VS [16–19]. Increasing evidence suggests that resting-state EEG coherence serves as a robust tool for quantifying the relationship between conscious awareness and cerebral information processing and provides more granular insight into differentiating between various levels of consciousness [20,21]. Patients who regained consciousness demonstrated higher levels of cortical functional connectivity in quantity and strength in a clinical trial assessing the prognosis of patients with DoC over a 3-month period [22]. Schorr *et al.* [23] proposed that the coherence between frontal and parietal regions serve as a predictive marker for dynamic shifts in consciousness states, such as recovery from VS-to-MCS with delta and theta in the parietal cortex showing high sensitivity and specificity in forecasting recovery in patients with VS.

It is indisputable that significant challenges remain in the diagnosis and management of DoC, primarily due to an insufficient understanding of the neurophysiologic mechanisms underlying consciousness. Therefore, a comprehensive analysis of EEG signals was performed in DoC patients with a focus on the whole-brain power spectral distribution, amplitude fluctuations within distinct frequency bands, and the functional state of brain connectivity in the resting state. By integrating these brain-machine data, a more cohesive model of the consciousness network within the brain was constructed. Furthermore, the most valuable EEG features related to consciousness were identified, thereby advancing the use of resting-state EEG in DoC. This approach will enhance the accuracy of diagnosis, enable better monitoring of therapeutic interventions, and facilitate the prediction of recovery in DoC patients.

2. Materials and Methods

2.1 Subjects

This study recruited a total of 90 patients with DoC from the Department of Rehabilitation Medicine of the Affiliated Hospital of Nantong University (Jiangsu, China). Due to issues, such as poor data quality and changes in clinical condition, 23 patients withdrew during the study. Ultimately, 67 patients were included in the analysis (19 with coma, 23 with VS, and 25 with MCS). The baseline characteristics of the sample are listed in Table 1.

All enrolled patients met the following inclusion criteria: (1) met the diagnostic criteria for DoC [6,24]; (2) >18 years of age; (3) DoC caused by various reasons, including both traumatic brain injury (TBI) and non-traumatic brain injury (NTBI). NTBI etiologies encompassed hypoxic-ischemic encephalopathy, cerebrovascular stroke, intracranial infection (e.g., encephalitis), and metabolic/toxic encephalopathy; and (4) informed consent was obtained from the subjects' legal guardian. The exclusion criteria were as follows: (1) history of neurologic or psychiatric illness; (2) presence of metal implants or implanted electronic brain medical devices, such as pacemakers; (3) history of cranioplasty with unhealed skull flap or severe scalp trauma, inability to place electrodes, or possible infection due to examination; (4) exposure to centrally acting medications within 24 h prior to EEG acquisition or within five

Table 1. Baseline characteristics of the sample.

Variables	Coma	VS	MCS	*p*
	n = 19	*n* = 23	*n* = 25	
Gender, n (%)				0.105
Male	9 (47.4%)	12 (52.2%)	19 (76.0%)	
Female	10 (52.6%)	11 (47.8%)	6 (24.0%)	
Age, years				0.944
Median (Q_l, Q_u)	64 (58.0, 71.0)	64 (56.0, 69.0)	64 (48.5, 74.5)	
Time since injury, months				0.099
Median (Q_l, Q_u)	2.0 (1.3, 2.4)	1.4 (1.1, 2.3)	1.3 (1.0, 1.9)	
Etiology				0.512
NTBI	10 (52.6%)	11 (47.8%)	9 (36.0%)	
TBI	9 (47.4%)	12 (52.2%)	16 (64.0%)	
Behavioral scale assessment				
Total score of CRS-R	2 (1, 3)	9 (7, 9)	12 (11, 14)	<0.001
Total score of GCS	4 (3, 5)	6 (4, 7)	11 (10, 11)	<0.001

VS, vegetative state; MCS, minimally conscious state; NTBI, non-traumatic brain injury; TBI, traumatic brain injury; CRS-R, coma recovery scale-revised; GCS, glasgow coma scale.

drug half-lives, whichever was longer, that are known to significantly alter EEG background activity or functional connectivity, including sedatives/anesthetics (e.g., propofol, benzodiazepines, dexmedetomidine), opioids, antipsychotics, antidepressants, antiepileptic drugs, or pharmacologic arousal agents (e.g., amantadine or zolpidem), as well as continuous infusions or regimens that were newly initiated or dose-adjusted during this period; (5) patients with combined multi-system and -organ dysfunction; (6) unstable vital signs (patients with a systolic BP $<$90 or $>$180 mmHg, heart rate $<$40 or $>$120 bpm, respiratory rate $<$8/min or ventilator-dependent, or SpO_2 $<$90% within 24 h pre-EEG were excluded); and (7) excessive motion artifacts (EEG epochs with an amplitude $>$75 µV, application of independent component analysis (ICA), or visual inspection by two technicians as motion artifacts).

The study was conducted under the Declaration of Helsinki of the World Medical Association and approved by the Ethics Committee of Nantong University Affiliated Hospital on 20 July 2024. The approval number for the study was 2024-K142-01. Before inclusion, the researcher fully informed the legal guardian of each patient about the study protocol and obtained informed consent, especially those in a coma state.

2.2 Clinical Assessment

Patients were systematically evaluated using the CRS-R and Glasgow Coma Scale (GCS) after a preliminary diagnosis of DoC [25–27]. Two trained therapists independently performed all assessments with discrepancies resolved through consensus. Three separate CRS-R and GCS evaluations were performed to accurately determine the patient's level of consciousness at least 5 d prior to the EEG assessment.

CRS-R systematically evaluates 6 functional domains (auditory, visual, motor, oromotor/verbal, communication, and arousal) using a 23-point hierarchical scale. Lower subscale scores suggest brainstem-mediated reflexive responses, while higher scores imply cortically-driven cognitive processing. As the gold-standard behavioral assessment for DoC, CRS-R demonstrates superior sensitivity in differentiating unresponsive wakefulness syndrome (UWS) from a MCS by detecting reproducible neurobehavioral markers, such as visual tracking [2].

GCS quantifies acute cerebral dysfunction through triaxial responsiveness, as follows: ocular (1–4); verbal (1–5); and motor (1–6). Total scores stratify injury severity, as follows: 15 (intact); 13–14 (mild); 9–12 (moderate); and 8 (coma/severe dysfunction) [28,29]. Serial GCS monitoring (hourly when $\leq$8) predicts secondary deterioration via a $\geq$2-point cumulative decline [29]. The verbal component is annotated as "T" with emphasis on non-verbal consciousness markers (e.g., visual tracking) for intubated patients. Assessments require exclusion of confounders (sedatives and hypoglycemia) [29]. Notably, GCS lacks specificity for chronic DoC subtypes, necessitating CRS-R supplementation to detect covert awareness [30].

2.3 EEG Recordings and Processing

Resting-state EEG data were collected from patients with three types of DoC. A 32-channel EEG (ZhenTec-NT1, ZhenTec Intelligent Technology Co., Ltd., Xi'an, Shaanxi, China) cap from a brain-computer interface (BCI) system was utilized. The electrodes were positioned in accordance with the internationally recognized 10–10 system [30]. The impedance of all electrodes was maintained below 10 kΩ. Each patient underwent a minimum of a 10-min resting-state EEG recording to facilitate the analysis of key EEG characteristics.

The pre-selected EEG data were pre-processed using MATLAB 2021a (The MathWorks Inc, Natick, MA, USA) and the EEGLAB toolbox (version 2022.1; Swartz Center for Computational Neuroscience, University of California San Diego, San Diego, CA, USA). The pre-processing steps were as follows: (1) electrode coordinate file was loaded and mapped to the corresponding electrode positions on the EEG cap (Gelfree-S3, Wuhan Greentek Pty. Ltd., Wuhan, Hubei, China); (2) a notch filter was applied using the ERPLAB filter to eliminate a 50-Hz power line interference; (3) band-pass filtering was performed between 1 and 45 Hz using a sixth-order Butterworth filter [31–33]; (4) Epochs with evident electromyographic or motion artifacts and non-EEG electrodes (e.g., electrooculogram) were excluded; (5) application of independent component analysis (ICA) to identify and remove the components related to physiologic artifacts, such as eye movements and electromyography; and (6) the average results of 30-channel electroencephalogram data.

2.4 Data Analysis

2.4.1 aEEG Center Amplitude (Median of Upper/Lower Margins)

The aEEG assesses brain electrical activity by real-time monitoring of EEG amplitude characteristics. This method typically involves computing the mean amplitude within specific EEG frequency bands and analyzing waveform trends. Raw EEG was band-pass filtered to the aEEG bandwidth (≈ 2–15 Hz) and time-compressed to generate the amplitude-integrated trace following standard methodology. We extracted the upper envelope (high amplitude) and lower envelope (low amplitude) of the EEG signal. Within each subject, the center amplitude was defined per channel as follows:

$$\text{center} = \frac{\text{upper} + \text{lower}}{2}$$

Where, upper and lower denote the time-median values of the aEEG margins over the full recording. We then aggregated across the 30 channels by taking the within-subject median, yielding a single whole-brain aEEG-center value per subject for group comparisons (Coma, VS, MCS) [34–36]. The primary analysis used Kruskal–Wallis test for independent groups with Dunn post hoc comparisons (all three pairwise contrasts).

2.4.2 Power Spectral Analysis

Power spectral analysis, which is a fundamental methodology for decomposing neural signals into constituent frequency components and quantifying the energy distribution, utilizes the fast Fourier transform (FFT) to convert EEG signals from the temporal domain to the frequency domain. Subsequently, squared amplitude values were calculated to generate power spectra. To enhance visual interpretability, power values are typically normalized using logarithmic decibel (dB) scaling via the following formula: dB = $10 \cdot \log_{10}$(power/reference). Spectral profiles systematically reveal energy distribution patterns across canonical frequency bands in electroencephalographic investigations, providing quantitative insights into cerebral oscillatory dynamics. Notably, healthy individuals typically exhibit prominent α-band power (8–13 Hz) over occipital regions during eyes-closed rest. However, individual variations exist. In contrast, consciousness-impaired patients frequently demonstrate marked α-power attenuation [30]. Analytical outcomes are visualized as spectrograms with dual-axis representations, as follows: frequency range (0–45 Hz) on the abscissa; and power intensity (dB) on the ordinate. Comparative analysis of spectral signatures across clinical states enables identification of consciousness-related pathologic patterns, including elevated θ/β power ratios and disrupted cross-frequency coupling profiles [7]. These spectral biomarkers complement multimodal assessments of DoC by objectively characterizing neurophysiologic aberrations in both resting-state and task-evoked conditions.

2.4.3 Whole-Brain Relative Power Distribution and Absolute Power Topographic Analysis

Relative power analysis quantitatively assesses cerebral electrophysiologic activity by evaluating the proportional contribution of specific frequency bands to total spectral power. Relative power analysis quantifies cerebral electrophysiologic activity by calculating the power spectral density (PSD) for each frequency band via Welch's periodogram, then normalizing the band power with respect to the total power to obtain relative power ratios. This normalization reduces inter-subject variability due to anatomic and technical factors with results often visualized as cortical heat maps, facilitating reliable cross-cohort spectral comparisons.

Furthermore, absolute power topographic mapping visualizes spatial-frequency abnormalities in DoC via 2D scalp projections derived from 3D data. The computational pipeline includes the following elements: (1) FFT-based PSD extraction; (2) spectral summation within clinically relevant bands (δ-γ); (3) dB conversion (dB = $10 \cdot \log_{10}$(P/Pref), where Pref denotes baseline power); (4) spatial interpolation (bilinear or radial basis function algorithms) for continuous scalp projections; and (5) color-coded visualization using standardized jet color maps. These biomarkers provided spatially resolved indices that may reveal DoC-related patterns with the EEGLAB topoplot function. This multimodal approach could enhance sensitivity in consciousness-level stratification and neuromodulation response assessment when integrated with aEEG metrics.

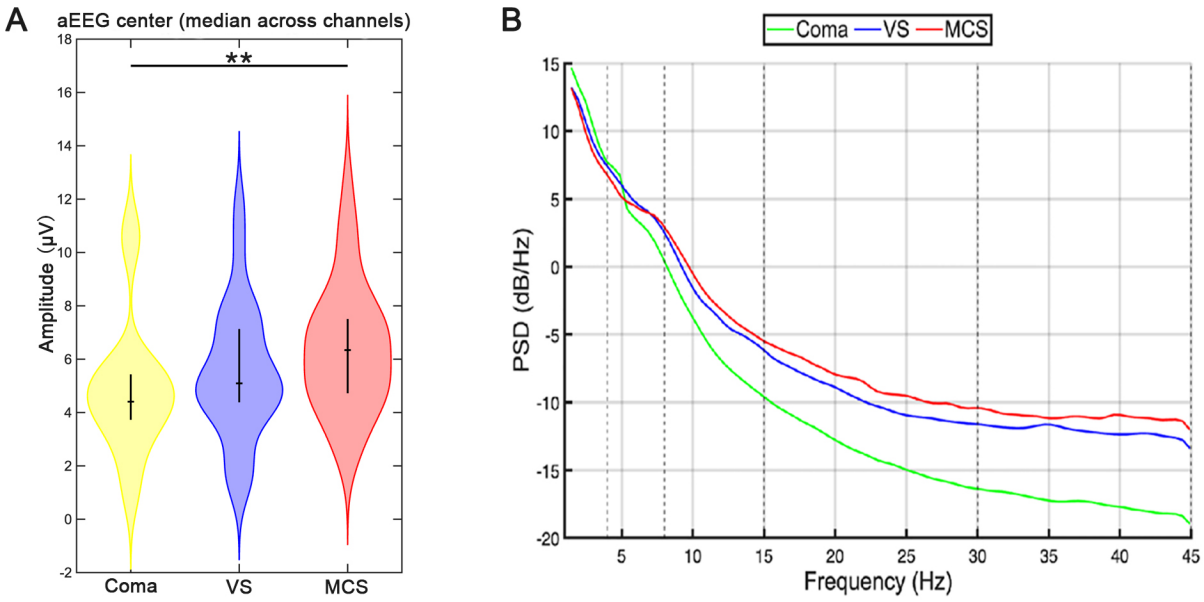

Fig. 1. Power spectrum and aEEG center amplitude of patients with DoC. The yellow, blue, and red columns in (A) correspond to the coma, VS, and MCS groups, respectively. The Dunn's *post hoc* test was used for intergroup comparison. $^{**}p < 0.01$ for intergroup comparison. (B) shows the comparison between the power spectrum analysis results of EEG data among the three groups and the dashed lines represent the boundaries of the standardized frequency bands. Green is for coma, blue is for VS, and red is for MCS. aEEG, amplitude-integrated electroencephalography; DoC, disorders of consciousness.

2.4.4 Weighted Phase Lag Index (wPLI)

The wPLI is an extension of the Phase Lag Index (PLI) that integrates a weighting mechanism. This modification provides several potential benefits, such as improved statistical sensitivity for detecting changes in consistent phase lead/lag between signals, enhanced robustness to additional noise sources, and a reduced impact of small phase differences. Consequently, wPLI may provide a more reliable estimate of the coupling strength of neural oscillations in the brain. The calculation method is outlined as follows:

$$\text{wPLI} = \frac{|\langle \Im(X) \rangle|}{\langle |\Im(X)| \rangle} = \frac{|\langle |\Im(X)| \, \text{sign}(\Im(X)) \rangle|}{\langle |\Im(X)| \rangle}$$

where, $\Im(X)$ represents the imaginary component of the cross-spectrum between $x_{(t)}$ and $y_{(t)}$. The value of wPLI ranges from 0–1. Values approaching 1 reflect a stable directional phase lead/lag, whereas values near zero indicate absence of a consistent phase-lagged relationship.

Functional connectivity metrics, including coherence and the wPLI, offer complementary approaches for mapping neural interactions. Coherence captures linear signal synchrony but is confounded by volume conduction artifacts. In contrast, wPLI improves specificity to phase-lagged coupling by weighting phase differences, which effectively suppresses the spurious synchronization arising from volume conduction [37]. In graph-theoretical analyses these metrics are used to define the edge weights of networks where nodes represent brain regions. The resulting connection strengths can be visualized as spatial patterns, aiding the identification of neuropathologic network reorganization. However, interpretation of these findings requires addressing methodologic constraints, including threshold selection biases, signal non-stationarity in wPLI estimation, and integration with structural connectivity data to resolve neurophysiologic ambiguities.

2.4.5 Statistical Analysis

Statistical analyses were performed using SPSS (Version 26.0, IBM Corp., Armonk, NY, USA) and MATLAB (R2021a, The MathWorks Inc., Natick, MA, USA) with an $\alpha = 0.05$. Categorical variables were summarized as a frequency (percentage). Group comparisons for categorical variables were made using a chi-square test. For continuous variables data with a normal distribution were analyzed by one-way analysis of variance (ANOVA) and expressed as the mean $\pm$ standard deviation; otherwise, the Kruskal–Wallis H test was used, with data presented as a median (IQR). If the ANOVA was significant, the Tukey-Kramer *post hoc* test was performed. Considering that multiple comparisons may increase type I errors, the Benjamini–Hochberg (BH) FDR was used to correct the main effect *p*-values and report the q-values (significance threshold q <0.05) (**Supplementary Tables 1,2**).

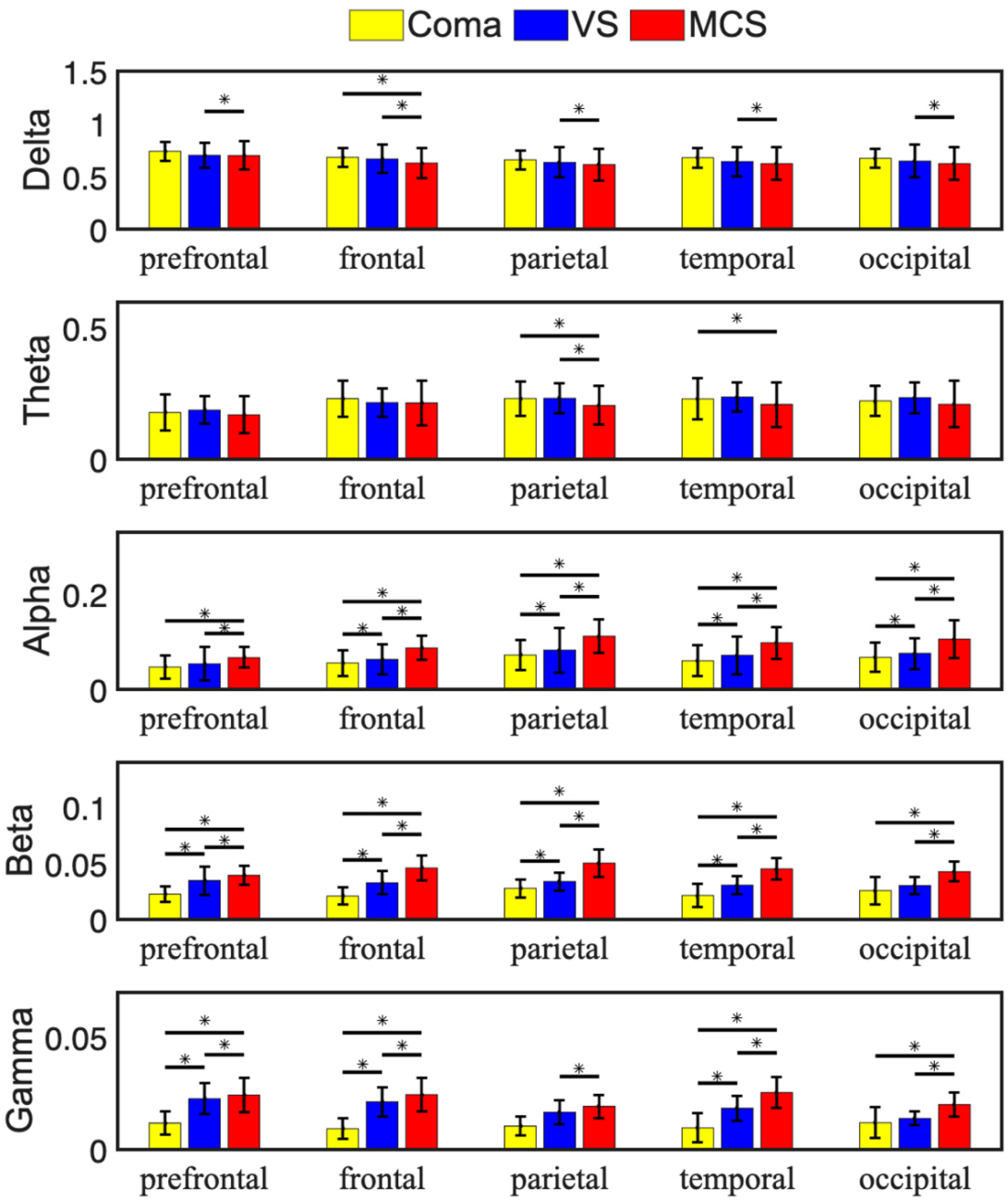

Fig. 2. Average relative EEG power of patients with DoC. The average data of three groups of patients with respect to different brain regions and frequency bands were compared. In the histogram, yellow, blue, and red represented coma, VS, and MCS groups, respectively. The error line represents the standard deviation within the group. The Tukey–Kramer test was performed on the data between each two groups when the results of the ANOVA were significant. *$p < 0.05$ for intergroup comparison. ANOVA, one-way analysis of variance.

3. Results

3.1 Comparison of aEEG Center Amplitude and Average EEG Power Spectra

The aEEG system quantifies the functional state of the brain by extracting the upper envelope (high amplitude) and lower envelope (low amplitude) of the EEG signal, then calculating the median values of upper- and lower-margin amplitudes [38]. The Dunn's *post hoc* test was performed between the groups (Coma–VS, Coma–MCS, and VS–MCS) when the Kruskal–Wallis test showed a significant result. The Kruskal–Wallis test was significant ($p = 0.02228$), and Dunn's *post hoc* test identified a significant Coma–MCS difference ($p = 0.02688$), with Coma–VS and VS–MCS remaining non-significant ($p = 0.6096$ and $p = 0.3649$, respectively) (Fig. 1A). Collectively, the between-group effect was primarily driven by the Coma vs. MCS contrast, with no significant differences observed for the other pair-

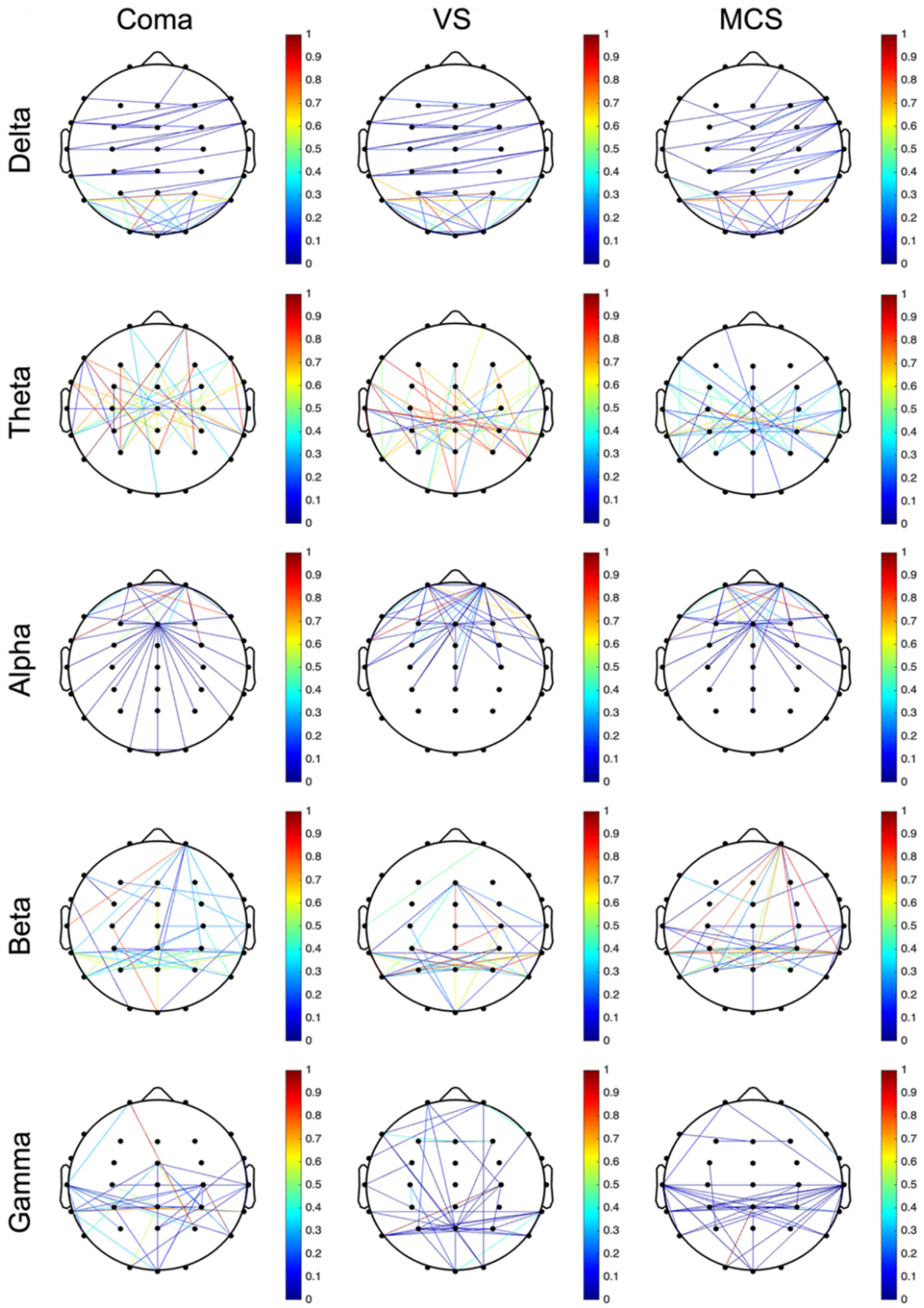

Fig. 3. wPLI-based functional connectivity matrices of brain regions across five frequency bands. Reflecting to the functional connectivity between different brain compartments, the nodes (Nodes) usually represent electrode positions arranged in a 10–10 system and the lines connecting the nodes are edges (Edges), which indicate the strength of connectivity as calculated by the wPLI. The deeper the red color, the stronger the intensity; the deeper the blue color, the weaker the intensity. The connection lines for intensities greater than the threshold were drawn using the 90th percentile as the threshold and marking it at the top of the image. wPLI, Weighted Phase Lag Index.

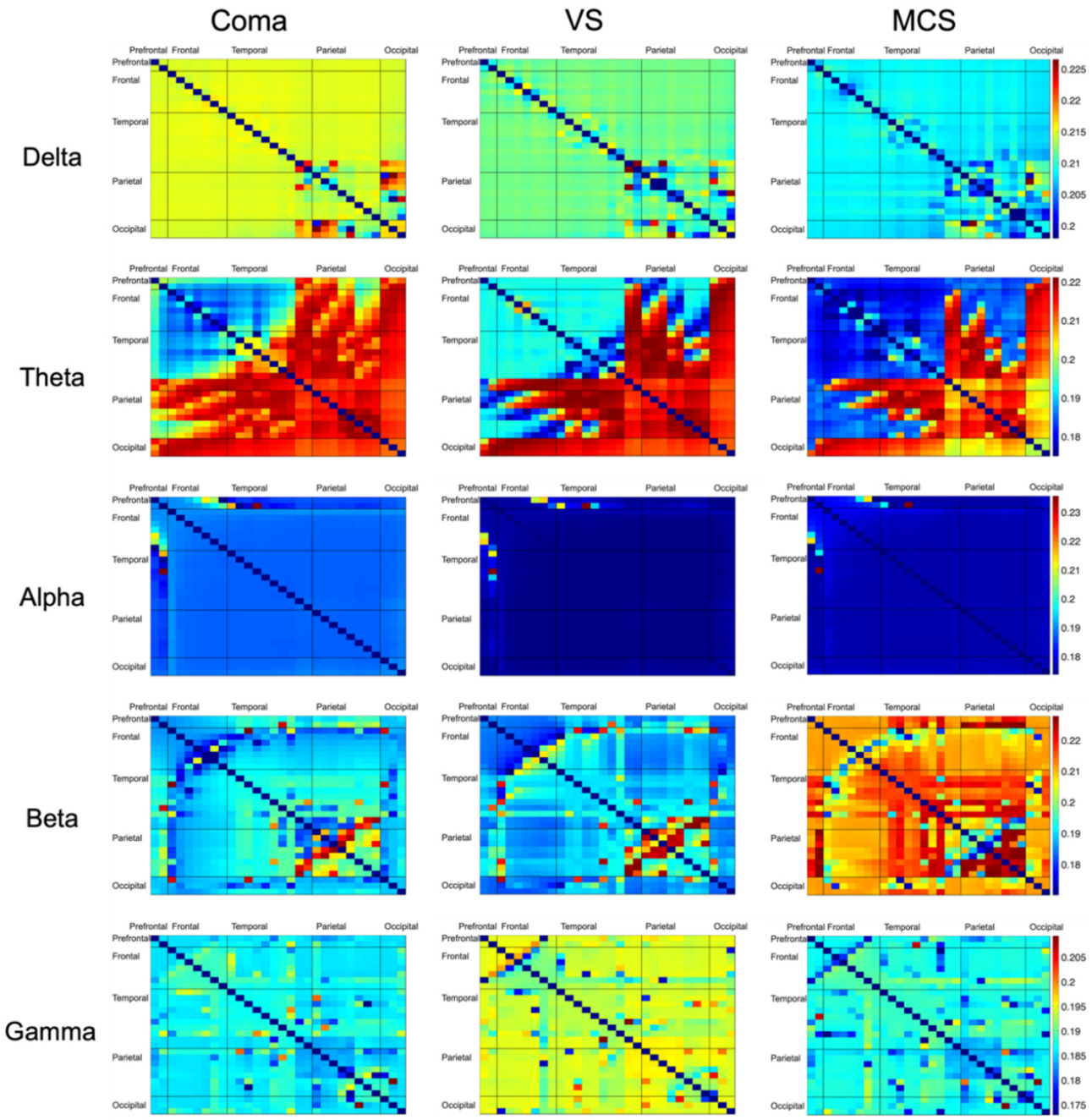

Fig. 4. Connectivity matrix of wPLI brain connections in different brain regions of patients with DoC. The connectivity matrix of wPLI brain connections reflects the connection characteristics and intensity in different frequency bands and the closer the value is to 1 (the closer the color is to red), the stronger the connection coherence between the two channels. Rows and columns represent brain regions in turn (prefrontal, frontal, temporal, parietal, and occipital).

ings. These findings indicated that while aEEG center amplitude can effectively distinguish coma from MCS, it may lack sufficient sensitivity to discern not only the distinctions between coma and VS, but also the more subtle ones between VS and MCS.

Systematic analysis of EEG power spectral characteristics in patients with DOC revealed distinct energy distribution patterns across frequency bands (Fig. 1B). The absolute power exhibited a descending gradient (coma > VS > MCS) in the delta band with the coma group showing the highest power and the MCS group showing the lowest power. Conversely, the coma group power decreased to the lowest level, while the MCS group power increased to the highest level in the theta band. The absolute power pattern reversed to MCS > VS > coma in the alpha, beta, and gamma bands.

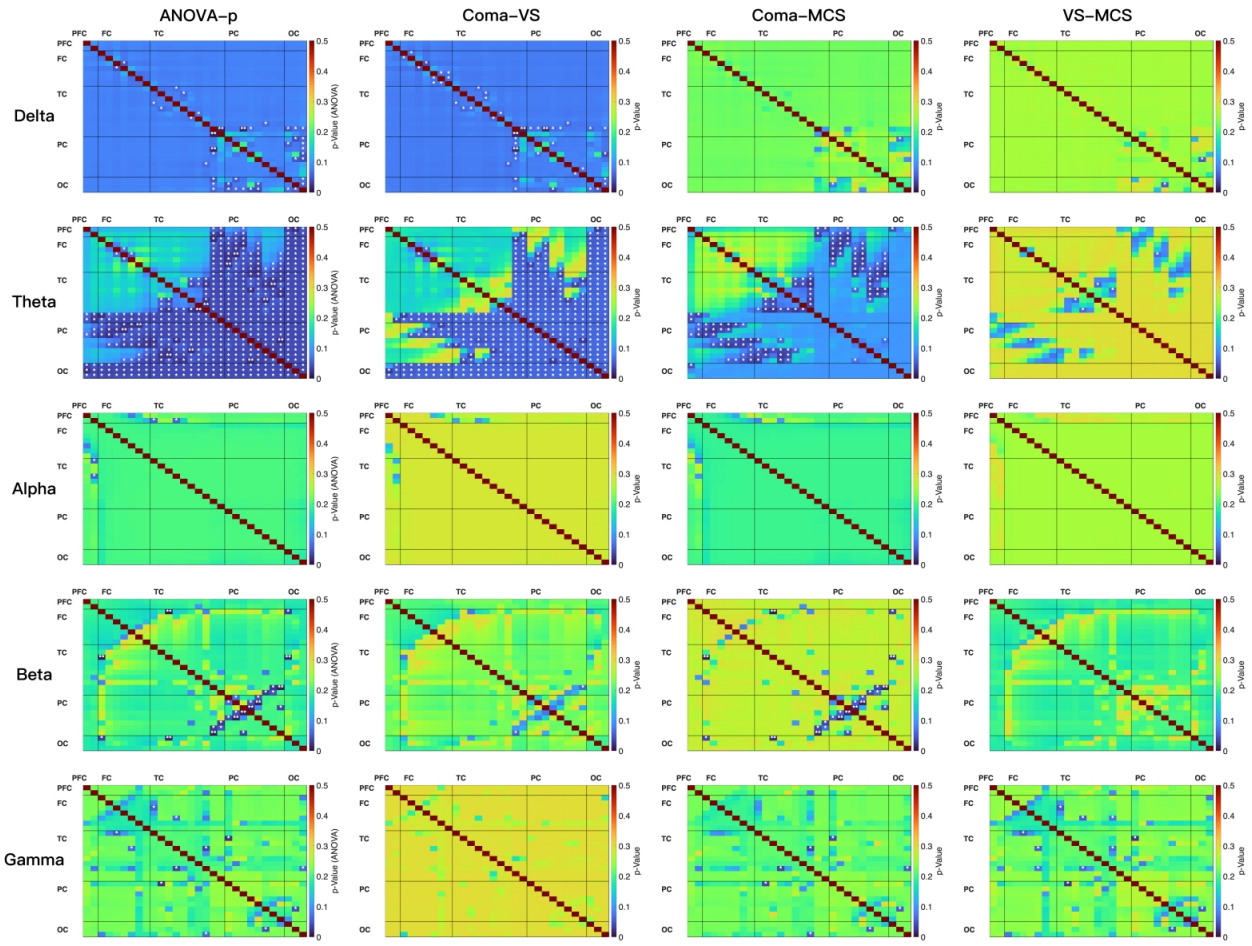

Fig. 5. Statistical analysis matrix of brain networks connectivity of patients with DoC. Edge-wise comparisons of functional connectivity indices were performed within each frequency band across three independent groups (coma, VS, and MCS). Connectivity strengths of the three groups were pooled (missing values were excluded) for each channel pair (upper triangle of the 30 × 30 matrix; 435 edges total) with each edge treated as an independent unit for intergroup testing (diagonal self-connections excluded). A one-way ANOVA was first applied to each edge to test the main group effect. Tukey–Kramer pairwise comparisons (coma–MCS, coma–VS, and VS–MCS) generated *p*-value matrix plots with a uniform color scale, overlaid brain region partition boundaries, and significant units marked by asterisks (*: $0.01 < p < 0.05$; **: $p < 0.01$).

3.2 Comparison of Relative Power Data of Each Brain Region

Relative power, a core quantitative indicator in EEG analysis, untangles the distribution characteristics of different band oscillatory energy within the total power spectrum [39] (Fig. 2; **Supplementary Tables 1,2**). Group differences in each frequency band were analyzed to clarify the frequency- and region-specific differences across DoC states, as follows. Significant differences were observed in the delta band between the VS and MCS groups across the entire brain. In addition, the coma and MCS groups exhibited significant differences within the frontal lobe. Significant differences were identified in the theta band between the coma and MCS groups in the parietal and temporal regions with differences between the VS and MCS groups (specifically in the parietal region). Significant differences were identified in the alpha band between the coma and MCS groups and between the VS and MCS groups in the prefrontal cortex. Furthermore, all pairwise comparisons among the three groups (coma, VS, and MCS) had significant differences across all other brain regions. Significant differences were observed in the beta band between the coma and MCS groups and between the VS and MCS groups within the occipital lobe. Moreover, all pairwise comparisons among the coma, VS, and MCS groups demonstrated significant differences across all other brain regions. Significant differences were noted in the gamma band between the VS and MCS groups in the parietal lobe. Significant differences were observed in the occipital lobe between the coma and MCS groups and between the VS and

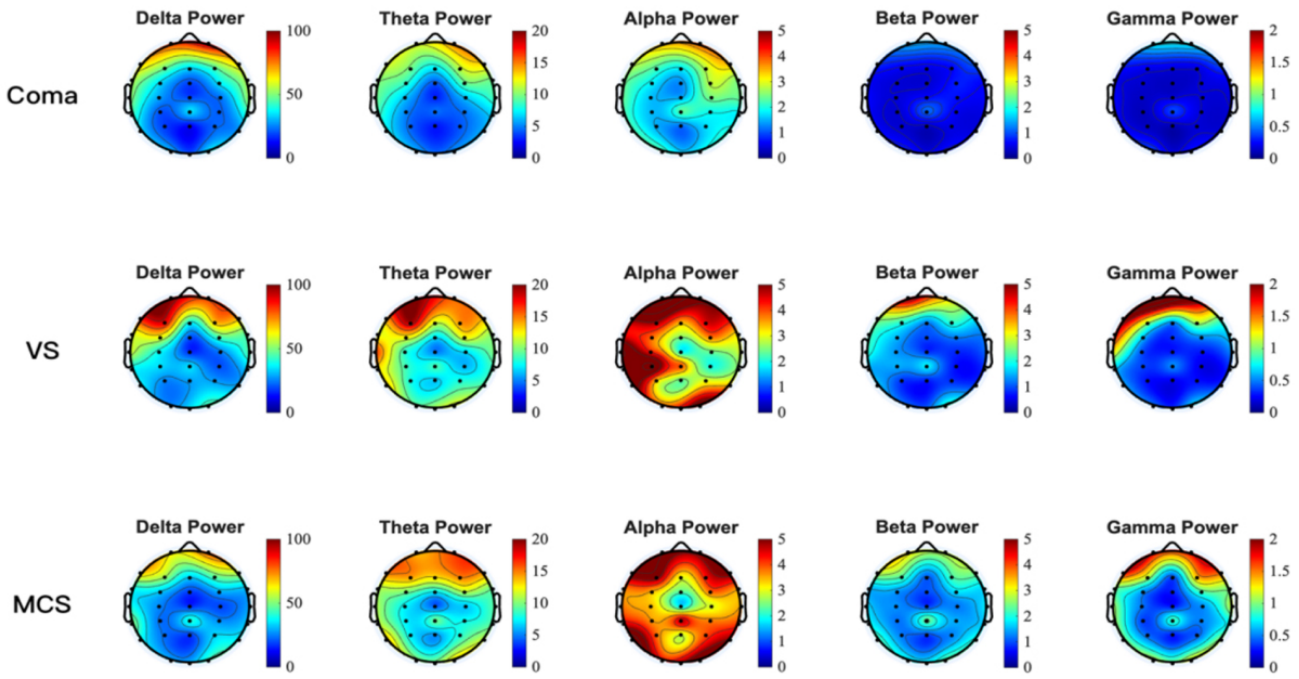

Fig. 6. Absolute power topographic maps of five rhythms in patients with DoC. Nodes typically represent electrode positions arranged in a 10–10 system. The deeper the red color, the higher the absolute power and the deeper the blue color, the lower the absolute power.

MCS groups. Moreover, all pairwise comparisons among the three groups demonstrated significant differences across the prefrontal, frontal, and temporal cortical regions.

3.3 Connectivity Analysis of Brain Network Based on wPLI

Functional connectivity of the brain refers to the synergistic relationship between different brain regions, reflecting collaboration in processing information [40]. The wPLI was used to reveal functional interaction patterns between different brain regions and systematically analyze functional brain network connectivity patterns in different frequency bands in three groups of patients to quantitatively characterize functional brain network connectivity [41,42] (Fig. 3).

All three groups showed dense connectivity in the delta band within the occipital lobe. Dense connectivity was observed in the theta band within the temporal, frontal, and parietal lobes across the three groups. The connectivity strength in the coma and VS groups was significantly higher than the MCS group with the VS group exhibiting the highest connectivity strength among the three. Dense connectivity was present in the alpha band within the bilateral parietal and temporal lobes across the three groups. In addition, the coma and MCS groups showed dense connectivity between the bilateral parietal, and temporal lobes and the right prefrontal cortex. The three groups demonstrated a radial connectivity pattern centered on the central brain region in the beta band. A diffuse connectivity pattern across multiple brain regions was observed in the gamma band.

3.4 Connectivity Matrix Analysis of Different Brain Regions Based on wPLI Connections

The connectivity matrix of wPLI brain network connectivity indices for different brain regions reflects the connectivity characteristics and strengths of the patients under different bands (Fig. 4) [43]. The connection characteristics of each band were systematically compared to describe the network recombination of specific frequencies [44]. In addition, statistical matrices of brain networks were plotted for patients with DoC and different consciousness levels across each frequency band (Fig. 5).

The overall connectivity strength among the three groups showed a gradually decreasing trend in the delta band (coma $>$ VS $>$ MCS) and there was a dense connectivity in the occipital lobe region. Dense connectivity was observed in the bilateral parietal lobes, bilateral occipital lobes, and between the parieto-occipital region and other brain regions across the three groups in the theta band with the VS group showing the strongest connectivity. Significant differences were detected between the coma and VS groups in the bilateral parietal lobes, bilateral occipital lobes, and between the parieto-occipital region and other brain regions as illustrated in Fig. 6. In addition, significant differences were identified between the coma and MCS groups in the connections between temporal parietal lobes, the parietal lobe and the prefrontal, frontal, and temporal lobes. The three groups exhibited a connection pattern in the alpha band, which was centered on the frontal lobe and the right prefrontal lobe with radiation to other brain regions. The three groups shared similar connectivity patterns

in the beta band with prominent connectivity in the bilateral parietal lobes. The MCS group exhibited the highest overall connectivity strength among the three groups and showed significant differences from the coma group in the parietal lobe. Interestingly, the VS group demonstrated the highest overall connectivity strength in the gamma band.

3.5 Distribution Characteristics of Absolute Power Topographic Maps in Different Frequency Bands

The absolute power topographic map utilizes spatial visualization techniques to untangle the regional distribution characteristics of EEG energy intensity within specific frequency bands [45]. The color gradient mapping intuitively reflects the absolute power of neural oscillations in different brain regions. Based on this method, the current study compared the whole-brain and regional absolute power topographic maps (Fig. 6) across various bands for the three groups of patients with DoC. Distinct patterns of absolute power were observed among the three patient groups across the frequency bands.

The absolute power topographies of different DoC states across five frequency bands revealed the following. There was no significant difference among the three groups in all five frequency bands. The high power of the three groups was mainly concentrated in the delta frequency band within the frontal lobe region. The high power of the coma group in the theta band was primarily localized to the prefrontal, bilateral frontal, and bilateral temporal regions. The VS and MCS groups demonstrated a generalized increase in absolute power compared to the coma group, which was accompanied by a more widespread distribution of these high-power areas. The elevated power of the coma group remained concentrated in the alpha band within the prefrontal area. The VS group showed enhanced activity extending to the prefrontal, bilateral frontal, bilateral temporal, and partial occipital regions. The MCS group, however, displayed a global increase in absolute power across the entire brain with the most extensive distribution of high-power regions. The distribution of high-power areas showed a gradually expanding pattern in the beta and gamma frequency bands from the coma, VS, and MCS groups. A pattern of increasing absolute power at the F3 electrode (left dorsolateral prefrontal cortex) was observed across multiple frequency bands, following the descriptive sequence: coma $<$ MCS $<$ VS.

4. Discussion

Recent studies have demonstrated that multidimensional EEG indicators can effectively distinguish patients' levels of consciousness and provide an important basis for clinical assessment and prognosis. Our analysis revealed characteristic electrophysiological patterns across different states of impaired consciousness. A significant difference in aEEG center values was observed between coma and MCS patients. In terms of relative spectral power, significant differences were found in the δ and γ bands between VS and MCS patients, while relative power in the α and β bands showed significant differences among coma, VS, and MCS groups. Regarding functional connectivity, parieto-occipital connectivity matrices in the theta band exhibited more pronounced differences between VS and coma patients. Notably, in absolute power topography, activity over the left DLPFC (electrode F3) remained consistently elevated across all groups, following a gradient of coma $<$ MCS $<$ VS.

The results of the current study aligned closely with the existing literature and further refined the spectrum of EEG features associated with different levels of consciousness. Significant intergroup differences in quantitative scores were detected. The low amplitude range in the coma group indicated a significant decrease in brain activity levels, which reflected a severe disruption of brain network integration [46]. The "Theory of Consciousness Index" proposed by Casali *et al*. [47] suggests that changes in conscious states may be accompanied by reorganization of some neural networks. This reorganization may manifest as the partial preservation of cortical-thalamic connections. Notably, while pediatric EEG studies typically use limited-channel setups due to cranial size constraints, this adult-focused investigation utilized high-density 30-channel EEG [48]. This approach compensated for the spatial resolution limitations inherent in low-channel configurations [49], thereby enabling precise characterization of the dynamic reorganization of the prefrontal-parietal network [50]. Even if overall functional connectivity weakens, connections in some key areas may persist. The medium amplitude observed in the VS group may reflect this partial preservation of cortical-thalamic connections, which align with the Casali perspective [47]. The highest amplitude observed in the MCS group was associated with the enhanced functional connectivity of the default mode network (DMN) [30]. Patients in the MCS state may exhibit limited consciousness or responsiveness, demonstrating some degree of reaction to certain external stimuli, such as sound or touch [51]. The aEEG data from the three groups in the current study showed significant differences and exhibited a change corresponding to the level of consciousness. This finding indicated that aEEG may be a useful quantitative indicator for assessing levels of consciousness. The thalamo-cortical network functional integrity model (ABCD model) is an EEG-based power spectral density classification system that assesses the functional integrity of the thalamo-cortical network through EEG dynamic characteristics [52]. The ABCD model is used to describe neural activity patterns in different states of consciousness, as proposed by Curley *et al*. [52] in a 2022 study. Type A is characterized by dominance in the delta band, reflecting a complete lack of cortical input, and is commonly observed in patients with severe brain injuries that disrupt thalamocortical connections [53]. The dominance of delta band

power in coma patients aligned with the "A-type power spectrum" described in the literature, which is characterized by a loss of integrity and reduced excitability, reflecting severe inhibition of brain function [52,54]. In contrast, the preservation and enhancement of high-frequency activity (alpha/beta/gamma) in the MCS group supported the theory in which restoration of consciousness depended on high-frequency oscillations [7,55]. In addition, the elevated power in the gamma frequency band within the MCS group may be linked to higher-order cognitive processing [56]. The aEEG and power spectrum characteristics aligned with the classic pattern of low-frequency dominance and high-frequency attenuation observed in patients with DoC.

The close correlation between the power distribution of different frequency bands in various brain regions and levels of consciousness was highly consistent with recent studies on the neural mechanisms of consciousness [7]. The coma group exhibited the highest relative power in the delta band across all brain regions among the three patient groups. This finding supported the classic conclusion that low-frequency oscillations serve as markers of conscious inhibition, suggesting that the pathomechanism may be related to the generalization of slow-wave activity due to disintegration of the thalamo-cortical loop. The difference in theta power in the parietal lobe suggests that this area has a crucial role in maintaining consciousness [57]. Engemann DA *et al.* [58] reported that alpha band power was one of the most prominently performing indicators for distinguishing MCS from UWS among more than 100 EEG recordings. Stefan *et al.* [14] reported the neural characteristics of enhanced alpha band activity and elevated beta coherence in patients with MCS through multidimensional EEG analysis, including power spectra, connectivity, and information entropy, which provided a reliable quantitative index for clinically differentiating between UWS and MCS. Based on our analysis, patients in the MCS group demonstrated significantly higher spectral power in the α and β bands across nearly all brain regions compared to the other groups. Elevated power in these frequency bands reflected the preserved cortical synchronization, functional network integration, and neurometabolic coupling capacity of MCS patients, making these features key biomarkers for differentiating states of consciousness [32]. Gamma oscillations are associated with higher-order cognitive processing and information binding across different brain regions [59]. The widespread enhancement of activities in these frequency bands in MCS patients may underpin the residual awareness and cognitive functions, such as the ability to intermittently follow commands. This finding aligns with previous research suggesting that high-frequency gamma activity is a neural correlate of conscious perception [30].

The brain functional connectivity patterns of three patient groups across different frequency bands was systematically analyzed based on wPLI. The five-band wPLI brain connectivity matrix (Fig. 5) for different brain regions revealed the dynamic reorganization characteristics of patients with varying levels of consciousness in large-scale brain network integration and dissociation. The connection strength in the delta frequency band increased as the level of consciousness decreased, which may be related to inhibition of the cortical-thalamus circuit and enhancement of slow-wave activity [60]. All three groups of patients showed strong posterior regional connectivity in the delta frequency band. Delta activity is a hallmark of deep sleep and severe brain injury. The predominant distribution in the occipital cortex may reflect deafferentation of the visual pathways and a generalized suppression of cortical function [61]. This pattern was consistently observed across the three groups, indicating that severe cortical dysfunction is a common pathologic basis for patients with DoC. A particularly intriguing finding emerged in the theta band. The VS group exhibited the strongest frontal-temporal-parietal connectivity in the theta frequency, surpassing that of the MCS group. This result challenges the simplistic linear model that "stronger connectivity equals higher level of consciousness" and supports the "over-activation of thalamocortical circuits" hypothesis. The highest theta connectivity in the VS group may reflect enhanced thalamic drive leading to pathologic synchronization between cortical regions, whereas the relatively lower theta connectivity in MCS patients suggests that the thalamocortical system is beginning to break free from this rigid synchrony, transitioning toward more flexible and complex dynamic activity [62]. This finding is consistent with several fMRI studies, which have reported that thalamic functional connectivity abnormalities in VS patients are even more severe than in coma patients [63]. The alpha-band connectivity pattern, which is centered on the frontal-right prefrontal regions, may underlie the network foundation that sustains a basic level of consciousness [43]. The dense connections in the beta band among temporal, parietal, and frontal areas observed in the VS and MCS groups could correspond to residual cognitive processing and self-awareness capacities [64]. These findings echo fMRI studies that report damage to the DMN and executive control networks in DoC [65]. Gamma-band activity is considered the neural basis for consciousness integration and the "binding problem" [66]. Only diffuse, disorganized gamma connectivity was observed among all patients with DoC, strongly suggesting that the breakdown of high-frequency connections may be a key neurophysiologic substrate for the loss of conscious content.

The analysis of EEG absolute power topography across the entire brain and different brain regions in the three patient groups under five EEG rhythms is essential. This study compared EEG characteristics across frequency bands in patients with coma, VS, and MCS using absolute power topographic maps. The ubiquitous elevation of delta power in the prefrontal regions is consistent with previous literature, potentially stemming from the desynchronization

of thalamocortical projections and the hyper-synchronous firing of cortical neurons [30,67]. VS and MCS patients demonstrated stronger power and more widespread brain involvement in the theta band compared to the coma group, which aligns with the role of theta oscillations in attention, memory, and network integration [68,69]. Some studies have indicated that the preservation of theta activity is associated with the recovery of consciousness. Theta activity enhancement in MCS patients may reflect the partial functional preservation of thalamocortical circuits and the default mode network [70]. Chennu *et al*. [30] reported that alpha power is positively correlated with the retention of default network function, supporting use of alpha power as a predictor of recovery of consciousness. De Koninck *et al*. [71] noted that transcranial alternating current stimulation improves the state of consciousness by enhancing alpha synchronization, suggesting that alpha activity in patients with MCS may reflect residual neuroplasticity. Prefrontal beta activity correlated with dorsal attentional network function. The VS and MCS groups exhibited oscillatory activity in the beta band that was concentrated in the frontal regions with significantly greater power than the coma group. Neural oscillations in the beta frequency band had a key role in frontal-specific activation associated with motor intention. The increase in parietal beta power in patients with MCS may reflect a capacity for sensorimotor integration [72]. Gamma power was low in all three groups but prefrontal localization was active in the MCS and VS groups, which is consistent with the general observation of high-frequency oscillatory suppression in DoC [73,74]. Notably, the high-power regions across all frequency bands involved the prefrontal lobes. Stender *et al*. [75] concluded that for every 10% increase in prefrontal metabolic rate, the probability of patients with MCS converting to conscious wakefulness increased 2.3-fold in the PET study. Specifically, the left DLPFC (corresponding to the F3 electrode) functions as a critical hub between the executive control network (ECN) and the DMN. The absolute power at the F3 electrode exhibits a consistent trend of coma $<$ MCS $<$ VS across all frequency bands in the three groups, which is in agreement with the findings herein that the higher power observed in the VS group may arise from network dysregulation leading to excessive synchronization [20].

EEG has made significant progress in the diagnosis and prognostic assessment of DoC, particularly in distinguishing between UWS/ VS and MCS. Toplutaş *et al*. [76] successfully distinguished between patients with VS and MCS by analyzing the duration, transition probabilities, and spatial topologic features of resting EEG microstates [76–79]. The EEG spatial-spectral gradient model developed by Colombo *et al*. [58] in combination with support vector machines, achieved a classification accuracy of 92% in cross-center validation, outperforming the traditional CRS-R, which has an accuracy of approximately 75%. In addition, Pan *et al.* [80] successfully achieved online consciousness detection for patients with DoC using a P300 brain-computer interface network, attaining a response accuracy of 68%. Portable EEG systems have made significant advances in ICUs and rehabilitation wards, including real-time microstate tracking through mobile-based algorithms, multimodal stimulation paradigms integrating auditory, pain, and visual stimuli to enhance covert consciousness detection by 15%, and the integration of EEG features with clinical data to develop automated prognostic prediction models using elastic net regression [78]. The current study used a systematic analysis of multi-dimensional EEG features to uncover the differences in neural mechanisms among patients with DoC at varying levels of consciousness. The aEEG exhibited an increase corresponding to levels of consciousness and the power of high-frequency bands significantly increased with recovery of consciousness, further elucidating the association between high-frequency activity and consciousness recovery [30]. The elevated gamma-band power in MCS aligns with the existing literature. Gamma oscillations are associated with feature binding, attention, and conscious perception, and preservation of gamma oscillations in MCS may indicate residual cognitive capacity [33]. The increase in gamma power observed herein might reflect partially preserved thalamocortical and frontoparietal circuits, which are critical for consciousness. While previous studies have employed aEEG threshold criteria similar to those used in this research [10]—thereby providing a methodological precedent—it should be noted that standardized adult-specific threshold criteria remain to be established. Against this backdrop, the current study represents a methodologic breakthrough by integrating multi-dimensional EEG features, analyzing mechanisms across frequency bands, and validating findings with networks [81]. This approach transcends the limitations of single biomarkers and constructs a multi-scale model for consciousness recovery. In the future combining real-time neurofeedback with closed-loop regulation technology is expected to advance the assessment of DoC toward precision medicine.

However, although this study has made some advancements in methodology and existing evidence indicates that the level of consciousness serves as the primary determinant of neurophysiologic changes, it is still necessary to acknowledge the existence of certain limitations. First, its sample size was relatively limited, restricting the generalizability of findings. Second, it only focused on EEG features without integrating other neuroimaging modalities or comprehensive clinical variables. Third, the single-center design may introduce selection bias, and the follow-up period was not detailed. Fourth, diverse etiologies of DoC were not fully controlle. Future studies should increase the sample size, integrate multimodal neuroimaging and clinical data, extend the follow-up period, and conduct more explicit subgroup analyses in order to further validate and optimize the proposed model.

5. Conclusions

In summary, multidimensional EEG contributed to distinguishing different degrees of DoC. The aEEG center amplitude effectively distinguishes MCS from coma patients; relative power in the δ and γ bands shows discriminatory significance between VS and MCS patients; relative power in the α and β bands enables differentiation among coma, VS, and MCS patients. Furthermore, the brain network connectivity matrix in the θ band over the parieto-occipital region exhibits more distinct features when distinguishing coma from VS patients. The absolute power topography of the left DLPFC also demonstrates potential for discriminating levels of impaired consciousness, further supporting the utility of multidimensional EEG features in clinical differentiation.

Multidimensional EEG biomarkers extend prior single-domain EEG approaches by offering a concise, multiparametric framework that complements behavioral assessments and refines diagnostic classification in DoC. Future integration into bedside monitoring systems and automated analysis could enhance diagnostic accuracy, prognostication, and treatment monitoring.

Availability of Data and Materials

The data presented in this study are available on request from the corresponding author.

Author Contributions

SL and JG designed the study. YHS, SYL, JWC, MYZ collected the data. WJY and JZ analyzed the data and prepared the figures. YHS, SYL, JZ, WJY, JWC, MYZ drafted the manuscript. SL and JG brought major revisions in significant proportions of the manuscript. All authors read and approved the final manuscript. All authors have participated sufficiently in the work and agreed to be accountable for all aspects of the work.

Ethics Approval and Consent to Participate

The study was conducted under the Declaration of Helsinki of the World Medical Association and approved by the Ethics Committee of the Affiliated Hospital of Nantong University. The approval number for the study was 2024-K142-01. Before inclusion, the researcher fully informed the legal guardian of each patient about the study protocol and obtained informed consent.

Acknowledgment

We would like to express our gratitude to all those who acted as peer reviewers, providing us with their valuable opinions and suggestions.

Funding

This work was supported by the Jiangsu Province Research Hospital, China [grant numbers YJXYY202204], Natural Science Foundation of Jiangsu Province, China [grant number BK20241839] and Jiangsu Commission of Health, China [grant number M2022052].

Conflict of Interest

The authors declare no conflict of interest.

Supplementary Material

Supplementary material associated with this article can be found, in the online version, at https://doi.org/10.31083/JIN44233.

References

[1] Giacino JT, Fins JJ, Laureys S, Schiff ND. Disorders of consciousness after acquired brain injury: the state of the science. Nature Reviews. Neurology. 2014; 10: 99–114. https://doi.org/10.1038/nrneurol.2013.279.

[2] Giacino JT, Kalmar K, Whyte J. The JFK Coma Recovery Scale-Revised: measurement characteristics and diagnostic utility. Archives of Physical Medicine and Rehabilitation. 2004; 85: 2020–2029. https://doi.org/10.1016/j.apmr.2004.02.033.

[3] Giacino JT, Schnakers C, Rodriguez-Moreno D, Kalmar K, Schiff N, Hirsch J. Behavioral assessment in patients with disorders of consciousness: gold standard or fool's gold? Progress in Brain Research. 2009; 177: 33–48. https://doi.org/10.1016/S0079-6123(09)17704-X.

[4] Owen AM, Coleman MR, Boly M, Davis MH, Laureys S, Pickard JD. Detecting awareness in the vegetative state. Science. 2006; 313: 1402. https://doi.org/10.1126/science.1130197.

[5] Giacino JT, Katz DI, Schiff ND, Whyte J, Ashman EJ, Ashwal S, *et al*. Comprehensive Systematic Review Update Summary: Disorders of Consciousness: Report of the Guideline Development, Dissemination, and Implementation Subcommittee of the American Academy of Neurology; the American Congress of Rehabilitation Medicine; and the National Institute on Disability, Independent Living, and Rehabilitation Research. Archives of Physical Medicine and Rehabilitation. 2018; 99: 1710–1719. https://doi.org/10.1016/j.apmr.2018.07.002.

[6] Kondziella D, Bender A, Diserens K, van Erp W, Estraneo A, Formisano R, *et al*. European Academy of Neurology guideline on the diagnosis of coma and other disorders of consciousness. European Journal of Neurology. 2020; 27: 741–756. https://doi.org/10.1111/ene.14151.

[7] Sitt JD, King JR, El Karoui I, Rohaut B, Faugeras F, Gramfort A, *et al*. Large scale screening of neural signatures of consciousness in patients in a vegetative or minimally conscious state. Brain. 2014; 137: 2258–2270. https://doi.org/10.1093/brain/awu141.

[8] Engemann DA, Raimondo F, King JR, Rohaut B, Louppe G, Faugeras F, *et al*. Robust EEG-based cross-site and cross-protocol classification of states of consciousness. Brain: a Journal of Neurology. 2018; 141: 3179–3192. https://doi.org/10.1093/brain/awy251.

[9] Toet MC, van der Meij W, de Vries LS, Uiterwaal CSPM, van Huffelen KC. Comparison between simultaneously recorded amplitude integrated electroencephalogram (cerebral function monitor) and standard electroencephalogram in neonates. Pediatrics. 2002; 109: 772–779. https://doi.org/10.1542/peds.109.5.772.

[10] Tian G, Qin K, Wu YM, Ji Z, Wang JX, Pan SY. Outcome prediction by amplitude-integrated EEG in adults with hypoxic ischemic encephalopathy. Clinical Neurology and Neurosurgery. 2012; 114: 585–589. https://doi.org/10.1016/j.clineuro.2011.12.011.

[11] Rossi Sebastiano D, Panzica F, Visani E, Rotondi F, Scaioli V, Leonardi M, *et al*. Significance of multiple neurophysiological measures in patients with chronic disorders of consciousness. Clinical Neurophysiology. 2015; 126: 558–564. https://doi.org/10.1016/j.clinph.2014.07.004.

[12] Klimesch W. EEG alpha and theta oscillations reflect cognitive and memory performance: a review and analysis. Brain Research. Brain Research Reviews. 1999; 29: 169–195. https://doi.org/10.1016/s0165-0173(98)00056-3.

[13] Naro A, Bramanti P, Leo A, Cacciola A, Bramanti A, Manuli A, *et al*. Towards a method to differentiate chronic disorder of consciousness patients' awareness: The Low-Resolution Brain Electromagnetic Tomography Analysis. Journal of the Neurological Sciences. 2016; 368: 178–183. https://doi.org/10.1016/j.jns.2016.07.016.

[14] Stefan S, Schorr B, Lopez-Rolon A, Kolassa IT, Shock JP, Rosenfelder M, *et al*. Consciousness Indexing and Outcome Prediction with Resting-State EEG in Severe Disorders of Consciousness. Brain Topography. 2018; 31: 848–862. https://doi.org/10.1007/s10548-018-0643-x.

[15] Piarulli A, Bergamasco M, Thibaut A, Cologan V, Gosseries O, Laureys S. EEG ultradian rhythmicity differences in disorders of consciousness during wakefulness. Journal of Neurology. 2016; 263: 1746–1760. https://doi.org/10.1007/s00415-016-8196-y.

[16] Cavinato M, Genna C, Manganotti P, Formaggio E, Storti SF, Campostrini S, *et al*. Coherence and Consciousness: Study of Fronto-Parietal Gamma Synchrony in Patients with Disorders of Consciousness. Brain Topography. 2015; 28: 570–579. https://doi.org/10.1007/s10548-014-0383-5.

[17] Wu DY, Cai G, Zorowitz RD, Yuan Y, Wang J, Song WQ. Measuring interconnection of the residual cortical functional islands in persistent vegetative state and minimal conscious state with EEG nonlinear analysis. Clinical Neurophysiology. 2011; 122: 1956–1966. https://doi.org/10.1016/j.clinph.2011.03.018.

[18] Leon-Carrion J, Leon-Dominguez U, Pollonini L, Wu MH, Frye RE, Dominguez-Morales MR, *et al*. Synchronization between the anterior and posterior cortex determines consciousness level in patients with traumatic brain injury (TBI). Brain Research. 2012; 1476: 22–30. https://doi.org/10.1016/j.brainres.2012.03.055.

[19] King JR, Sitt JD, Faugeras F, Rohaut B, El Karoui I, Cohen L, *et al*. Information sharing in the brain indexes consciousness in noncommunicative patients. Current Biology. 2013; 23: 1914–1919. https://doi.org/10.1016/j.cub.2013.07.075.

[20] Lehembre R, Marie-Aurélie B, Vanhaudenhuyse A, Chatelle C, Cologan V, Leclercq Y, *et al*. Resting-state EEG study of comatose patients: a connectivity and frequency analysis to find differences between vegetative and minimally conscious states. Functional Neurology. 2012; 27: 41–47.

[21] Naro A, Bramanti A, Leo A, Cacciola A, Manuli A, Bramanti P, *et al*. Shedding new light on disorders of consciousness diagnosis: The dynamic functional connectivity. Cortex. 2018; 103: 316–328. https://doi.org/10.1016/j.cortex.2018.03.029.

[22] Fingelkurts AA, Fingelkurts AA, Bagnato S, Boccagni C, Galardi G. Prognostic value of resting-state electroencephalography structure in disentangling vegetative and minimally conscious states: a preliminary study. Neurorehabilitation and Neural Repair. 2013; 27: 345–354. https://doi.org/10.1177/1545968312469836.

[23] Schorr B, Schlee W, Arndt M, Bender A. Coherence in resting-state EEG as a predictor for the recovery from unre-sponsive wakefulness syndrome. Journal of Neurology, 2016; 263: 937-953. https://doi.org/10.1007/s00415-016-8084-5.

[24] Giacino JT, Katz DI, Schiff ND, Whyte J, Ashman EJ, Ashwal S, *et al*. Practice guideline update recommendations summary: Disorders of consciousness: Report of the Guideline Development, Dissemination, and Implementation Subcommittee of the American Academy of Neurology; the American Congress of Rehabilitation Medicine; and the National Institute on Disability, Independent Living, and Rehabilitation Research. Neurology. 2018; 91: 450–460. https://doi.org/10.1212/WNL.0000000000005926.

[25] Teasdale G, Jennett B. Assessment of coma and impaired consciousness. A practical scale. Lancet. 1974; 2: 81–84. https://doi.org/10.1016/s0140-6736(74)91639-0.

[26] Seel RT, Sherer M, Whyte J, Katz DI, Giacino JT, Rosenbaum AM, et al. Assessment scales for disorders of consciousness: evidence-based recommendations for clinical practice and research. Archives of physical medicine and rehabilitation. 2010, 91: 1795–1813. https://doi.org/10.1016/j.apmr.2010.07.218.

[27] Teasdale G, Maas A, Lecky F, Manley G, Stocchetti N, Murray G. The Glasgow Coma Scale at 40 years: standing the test of time. The Lancet. 2014; 13: 844–854. https://doi.org/10.1016/s1474-4422(14)70120-6.

[28] Kebapçı A, Dikeç G, Topçu S. Interobserver Reliability of Glasgow Coma Scale Scores for Intensive Care Unit Patients. Critical Care Nurse. 2020; 40: e18–e26. https://doi.org/10.4037/ccn2020200.

[29] Carney N, Totten AM, O'Reilly C, Ullman JS, Hawryluk GWJ, Bell MJ, *et al*. Guidelines for the Management of Severe Traumatic Brain Injury, Fourth Edition. Neurosurgery. 2017; 80: 6–15. https://doi.org/10.1227/NEU.0000000000001432.

[30] Chennu S, Finoia P, Kamau E, Allanson J, Williams GB, Monti MM, *et al*. Spectral signatures of reorganised brain networks in disorders of consciousness. PLoS Computational Biology. 2014; 10: e1003887. https://doi.org/10.1371/journal.pcbi.1003887.

[31] Rizkallah J, Annen J, Modolo J, Gosseries O, Benquet P, Mortaheb S, *et al*. Decreased integration of EEG source-space networks in disorders of consciousness. NeuroImage. Clinical. 2019; 23: 101841. https://doi.org/10.1016/j.nicl.2019.101841.

[32] Bai Y, Lin Y, Ziemann U. Managing disorders of consciousness: the role of electroencephalography. Journal of Neurology. 2021; 268: 4033–4065. https://doi.org/10.1007/s00415-020-10095-z.

[33] Bai Y, Xia X, Liang Z, Wang Y, Yang Y, He J, *et al*. Frontal Connectivity in EEG Gamma (30–45 Hz) Respond to Spinal Cord Stimulation in Minimally Conscious State Patients. Frontiers in Cellular Neuroscience. 2017; 11: 177. https://doi.org/10.3389/fncel.2017.00177.

[34] Kato T, Sugiyama Y, Tsuji T, Hayashi S, Natsume J, Okumura A. Differences in amplitude among electrode locations on amplitude-integrated electroencephalograms in preterm infants. Pediatric Research. 2012; 72: 57–62. https://doi.org/10.1038/pr.2012.50.

[35] Vesoulis ZA, Paul RA, Mitchell TJ, Wong C, Inder TE, Mathur AM. Normative amplitude-integrated EEG measures in preterm infants. Journal of Perinatology. 2015; 35: 428–433. https://doi.org/10.1038/jp.2014.225.

[36] Greve S, Brensing P, Paul L, Dohna-Schwake C, Wichlacz J, Felderhoff-Mueser U, *et al*. Systematically lower aEEG amplitude values in neurologically healthy children using an automated algorithm compared to a semi-manual method. Frontiers in Neurology. 2025; 16: 1562580. https://doi.org/10.3389/fneur.2025.1562580.

[37] Vinck M, Oostenveld R, van Wingerden M, Battaglia F, Pennartz CMA. An improved index of phase-synchronization for electrophysiological data in the presence of volume-conduction, noise and sample-size bias. NeuroImage. 2011; 55: 1548–1565. https://doi.org/10.1016/j.neuroimage.2011.01.055.

[38] Toet MC, Hellström-Westas L, Groenendaal F, Eken P, de Vries LS. Amplitude integrated EEG 3 and 6 hours after birth in full term neonates with hypoxic-ischaemic encephalopathy. Archives of Disease in Childhood. Fetal and Neonatal Edition.

1999; 81: F19–F23. https://doi.org/10.1136/fn.81.1.f19.
[39] Lin A, Liu KKL, Bartsch RP, Ivanov PC. Dynamic network interactions among distinct brain rhythms as a hallmark of physiologic state and function. Communications Biology. 2020; 3: 197. https://doi.org/10.1038/s42003-020-0878-4.
[40] Friston KJ. Functional and effective connectivity: a review. Brain Connectivity. 2011; 1: 13–36. https://doi.org/10.1089/brain.2011.0008.
[41] Zhang R, Zhang L, Guo Y, Shi L, Gao J, Wang X, *et al*. Effects of High-Definition Transcranial Direct-Current Stimulation on Resting-State Functional Connectivity in Patients With Disorders of Consciousness. Frontiers in Human Neuroscience. 2020; 14: 560586. https://doi.org/10.3389/fnhum.2020.560586.
[42] Stam CJ, Nolte G, Daffertshofer A. Phase lag index: assessment of functional connectivity from multi channel EEG and MEG with diminished bias from common sources. Human Brain Mapping. 2007; 28: 1178–1193. https://doi.org/10.1002/hbm.20346.
[43] Vanhaudenhuyse A, Noirhomme Q, Tshibanda LJF, Bruno MA, Boveroux P, Schnakers C, *et al*. Default network connectivity reflects the level of consciousness in non-communicative brain-damaged patients. Brain. 2010; 133: 161–171. https://doi.org/10.1093/brain/awp313.
[44] Park YH, Cha J, Bourakova V, Lee JM. Frequency specific contribution of intrinsic connectivity networks to the integration in brain networks. Scientific Reports. 2019; 9: 4072. https://doi.org/10.1038/s41598-019-40699-z.
[45] Alreshidi I, Moulitsas I, Jenkins KW. Multimodal Approach for Pilot Mental State Detection Based on EEG. Sensors. 2023; 23: 7350. https://doi.org/10.3390/s23177350.
[46] Pavel B. Important issues in coma and neuromonitoring. In Erbay RH (ed.) Current Topics in Intensive Care Medicine (pp. 41–58). InTech: Rijeka. 2018. https://doi.org/10.5772/intechopen.71644.
[47] Casali AG, Gosseries O, Rosanova M, Boly M, Sarasso S, Casali KR, *et al*. A theoretically based index of consciousness independent of sensory processing and behavior. Science Translational Medicine. 2013; 5: 198ra105. https://doi.org/10.1126/scitranslmed.3006294.
[48] Benedetti GM, Guerriero RM, Press CA. Review of noninvasive neuromonitoring modalities in children II: EEG, qEEG. Neurocritical Care. 2023; 39: 618–638. https://doi.org/10.1007/s12028-023-01686-5.
[49] Lachaux JP, Rodriguez E, Martinerie J, Varela FJ. Measuring phase synchrony in brain signals. Human Brain Mapping. 1999; 8: 194–208. https://doi.org/10.1002/(sici)1097-0193(1999)8:4<194::aid-hbm4>3.0.co;2-c.
[50] Cohen MX, van Gaal S. Dynamic interactions between large-scale brain networks predict behavioral adaptation after perceptual errors. Cerebral Cortex. 2013; 23: 1061–1072. https://doi.org/10.1093/cercor/bhs069.
[51] Annen J, Frasso G, van der Lande GJM, Bonin EAC, Vitello MM, Panda R, *et al*. Cerebral electrometabolic coupling in disordered and normal states of consciousness. Cell Reports. 2023; 42: 112854. https://doi.org/10.1016/j.celrep.2023.112854.
[52] Curley WH, Bodien YG, Zhou DW, Conte MM, Foulkes AS, Giacino JT, *et al*. Electrophysiological correlates of thalamocortical function in acute severe traumatic brain injury. Cortex. 2022; 152: 136–152. https://doi.org/10.1016/j.cortex.2022.04.007.
[53] Andraus MEC, Alves-Leon SV. Non-epileptiform EEG abnormalities: an overview. Arquivos De Neuro-Psiquiatria. 2011; 69: 829–835. https://doi.org/10.1590/s0004-282x2011000600020.
[54] Egawa S, Ader J, Claassen J. Recovery of consciousness after acute brain injury: a narrative review. Journal of Intensive Care. 2024; 12: 37. https://doi.org/10.1186/s40560-024-00749-9.
[55] Duszyk-Bogorodzka A, Zieleniewska M, Jankowiak-Siuda K. Brain Activity Characteristics of Patients With Disorders of Consciousness in the EEG Resting State Paradigm: A Review. Frontiers in Systems Neuroscience. 2022; 16: 654541. https://doi.org/10.3389/fnsys.2022.654541.
[56] Mangia AL, Pirini M, Simoncini L, Cappello A. A feasibility study of an improved procedure for using EEG to detect brain responses to imagery instruction in patients with disorders of consciousness. PLoS ONE. 2014; 9: e99289. https://doi.org/10.1371/journal.pone.0099289.
[57] Laureys S. The neural correlate of (un)awareness: lessons from the vegetative state. Trends in Cognitive Sciences. 2005; 9: 556–559. https://doi.org/10.1016/j.tics.2005.10.010.
[58] Engemann DA, Raimondo F, King JR, Rohaut B, Louppe G, Faugeras F, *et al*. Robust EEG-based cross-site and cross-protocol classification of states of consciousness. Brain. 2018; 141: 3179-3192. https://doi.org/10.1093/brain/awy251.
[59] Fernández-Ruiz A, Schomburg EW. The rules of entrainment: are CA1 gamma oscillations externally imposed or locally governed? The Journal of Neuroscience. 2013; 33: 19045–19047. https://doi.org/10.1523/JNEUROSCI.4151-13.2013.
[60] Raveendran S, S K, A G R, Kenchaiah R, Sahoo J, Kumar S, *et al*. Functional connectivity in EEG: a multiclass classification approach for disorders of consciousness. Frontiers in Neuroscience. 2025; 19: 1550581. https://doi.org/10.3389/fnins.2025.1550581.
[61] LaBarbera V, Nie D. Occipital intermittent rhythmic delta activity (OIRDA) in pediatric focal epilepsies: A case series. Epilepsy & Behavior Reports. 2021; 16: 100472. https://doi.org/10.1016/j.ebr.2021.100472.
[62] Weng L, Xie Q, Zhao L, Zhang R, Ma Q, Wang J, *et al*. Abnormal structural connectivity between the basal ganglia, thalamus, and frontal cortex in patients with disorders of consciousness. Cortex. 2017; 90: 71–87. https://doi.org/10.1016/j.cortex.2017.02.011.
[63] Crone JS, Lutkenhoff ES, Bio BJ, Laureys S, Monti MM. Testing Proposed Neuronal Models of Effective Connectivity Within the Cortico-basal Ganglia-thalamo-cortical Loop During Loss of Consciousness. Cerebral Cortex. 2017; 27: 2727–2738. https://doi.org/10.1093/cercor/bhw112.
[64] Gong A, Wang Q, Guo Q, Yang Y, Chen X, Hu X, *et al*. Variability of large timescale functional networks in patients with disorders of consciousness. Frontiers in Neurology. 2024; 15: 1283140. https://doi.org/10.3389/fneur.2024.1283140.
[65] Fernández-Espejo D, Soddu A, Cruse D, Palacios EM, Junque C, Vanhaudenhuyse A, *et al*. A role for the default mode network in the bases of disorders of consciousness. Annals of Neurology. 2012; 72: 335–343. https://doi.org/10.1002/ana.23635.
[66] Singer W. Synchronization of cortical activity and its putative role in information processing and learning. Annual Review of Physiology. 1993; 55: 349–374. https://doi.org/10.1146/annurev.ph.55.030193.002025.
[67] Frohlich J, Toker D, Monti MM. Consciousness among delta waves: a paradox? Brain. 2021; 144: 2257–2277. https://doi.org/10.1093/brain/awab095.
[68] Fingelkurts AA, Fingelkurts AA, Bagnato S, Boccagni C, Galardi G. Life or death: prognostic value of a resting EEG with regards to survival in patients in vegetative and minimally conscious states. PLoS ONE. 2011; 6: e25967. https://doi.org/10.1371/journal.pone.0025967.
[69] Landsness E, Bruno MA, Noirhomme Q, Riedner B, Gosseries O, Schnakers C, *et al*. Electrophysiological correlates of behavioural changes in vigilance in vegetative state and minimally conscious state. Brain. 2011; 134: 2222–2232. https://doi.org/10.1093/brain/awr152.
[70] Bonfiglio L, Piarulli A, Olcese U, Andre P, Arrighi P, Frisoli A, *et al*. Spectral parameters modulation and source localiza-

tion of blink-related alpha and low-beta oscillations differentiate minimally conscious state from vegetative state/unresponsive wakefulness syndrome. PLoS ONE. 2014; 9: e93252. https://doi.org/10.1371/journal.pone.0093252.

[71] De Koninck BP, Brazeau D, Deshaies AA, Briand MM, Maschke C, Williams V, *et al*. Modulation of brain activity in brain-injured patients with a disorder of consciousness in intensive care with repeated 10-Hz transcranial alternating current stimulation (tACS): a randomised controlled trial protocol. BMJ Open. 2024; 14: e078281. https://doi.org/10.1136/bmjopen-2023-078281.

[72] Peng J, Zikereya T, Shao Z, Shi K. The neuromechanical of Beta-band corticomuscular coupling within the human motor system. Frontiers in Neuroscience. 2024; 18: 1441002. https://doi.org/10.3389/fnins.2024.1441002.

[73] Hong SL, Rebec GV. A new perspective on behavioral inconsistency and neural noise in aging: compensatory speeding of neural communication. Frontiers in Aging Neuroscience. 2012; 4: 27. https://doi.org/10.3389/fnagi.2012.00027.

[74] Georgescu EL, Georgescu IA, Zahiu CDM, Ştеopoaie AR, Morozan VP, Pană AŞ, *et al*. Oscillatory Cortical Activity in an Animal Model of Dystonia Caused by Cerebellar Dysfunction. Frontiers in Cellular Neuroscience. 2018; 12: 390. https://doi.org/10.3389/fncel.2018.00390.

[75] Stender J, Mortensen KN, Thibaut A, Darkner S, Laureys S, Gjedde A, *et al*. The Minimal Energetic Requirement of Sustained Awareness after Brain Injury. Current Biology. 2016; 26: 1494–1499. https://doi.org/10.1016/j.cub.2016.04.024.

[76] Toplutaş E, Aydın F, Hanoğlu L. EEG Microstate Analysis in Patients with Disorders of Consciousness and Its Clinical Significance. Brain Topography. 2024; 37: 377–387. https://doi.org/10.1007/s10548-023-00939-y.

[77] Yu F, Gao Y, Li F, Zhang X, Hu F, Jia W, *et al*. Resting-state EEG microstates as electrophysiological biomarkers in post-stroke disorder of consciousness. Frontiers in Neuroscience. 2023; 17: 1257511. https://doi.org/10.3389/fnins.2023.1257511.

[78] Liuzzi P, Mannini A, Hakiki B, Campagnini S, Romoli AM, Draghi F, *et al*. Brain microstate spatio-temporal dynamics as a candidate endotype of consciousness. NeuroImage. Clinical. 2024; 41: 103540. https://doi.org/10.1016/j.nicl.2023.103540.

[79] Ling Y, Wen X, Tang J, Tao Z, Sun L, Xin H, *et al*. Effect of topographic comparison of electroencephalographic microstates on the diagnosis and prognosis prediction of patients with prolonged disorders of consciousness. CNS Neuroscience & Therapeutics. 2024; 30: e14421. https://doi.org/10.1111/cns.14421.

[80] Pan J, Xie Q, Qin P, Chen Y, He Y, Huang H, *et al*. Prognosis for patients with cognitive motor dissociation identified by brain-computer interface. Brain. 2020; 143: 1177–1189. https://doi.org/10.1093/brain/awaa026.

[81] Wutzl B, Golaszewski SM, Leibnitz K, Langthaler PB, Kunz AB, Leis S, *et al*. Narrative Review: Quantitative EEG in Disorders of Consciousness. Brain Sciences. 2021; 11: 697. https://doi.org/10.3390/brainsci11060697.